

# Supporting Information:

## Modulating and addressing interactions in polymer colloids using light

Emily W. Gehrels,<sup>†</sup> Ellen D. Klein,<sup>‡</sup> and Vinothan N. Manoharan<sup>\*,†,‡</sup>

<sup>†</sup>*Harvard John A. Paulson School of Engineering and Applied Sciences, Harvard  
University, Cambridge, Massachusetts 02138, USA.*

<sup>‡</sup>*Department of Physics, Harvard University, Cambridge, Massachusetts 02138, USA*

E-mail: vnm@seas.harvard.edu

### S1 DNA Sequences

DNA oligonucleotides are ordered from IDT with a 5' Dibenzocyclooctyne (DBCO) modification and with HPLC purification. The specific sequence used for the experiments presented in this article is self-complementary (5' - /5DBCOTEG/ - (T<sub>16</sub>) - CGCG - 3').

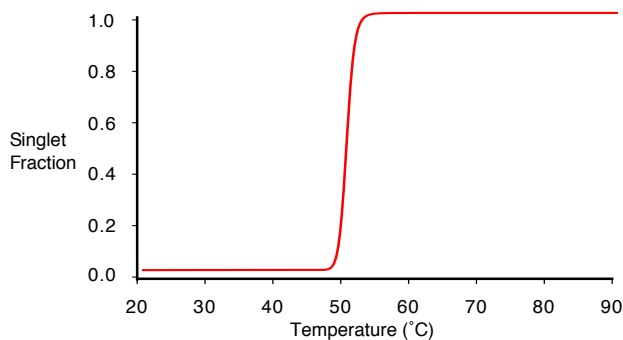


Figure S1: Plot of a typical theoretical singlet fraction curve for DNA-coated particles, calculated using the method described in Ref. S1.

## S2 Functionalizing particles with DNA

To functionalize the particles, we use a modified version of the protocol from Ref. S2. We modify PS-*b*-PEO with an azide group as described in the reference. We then mix 240  $\mu\text{L}$  of 417  $\mu\text{M}$  PS-*b*-PEO- $\text{N}_3$  in deionized (DI) water with 120  $\mu\text{L}$  Tetrahydrofuran (THF, Sigma) and 3  $\mu\text{L}$  toluene (anhydrous, Sigma-Aldrich) saturated with dye (Oil Blue N, 96%, Sigma-Aldrich or Oil Red O, BSC certified, Sigma-Aldrich). Finally we add 40  $\mu\text{L}$  of 1  $\mu\text{m}$  sulfate-modified polystyrene particles (Molecular Probes) that have been washed into 1x TE buffer, suspended to 10% v/v, and sonicated. The suspension is shaken at room temperature for 30 min. After shaking, an excess of DI water is added to the suspension to decrease the fraction of THF below 10%. We then heat the suspension to 70  $^\circ\text{C}$  for 1 h to evaporate the THF. The azide functionalized particles (PS-PS-*b*-PEO- $\text{N}_3$ ) are then washed several times in DI water.

Any dye that is soluble in toluene and polystyrene but insoluble in water can be used to dye particles in this way. The absorption spectra for the two dyes used in this paper are shown in Figure S2. The two dyes are suspended in toluene at 0.066% of the concentration at which the dye begins to precipitate, and their spectra are collected on a NanoDrop UV-Visible Spectrometer (Thermo Fisher Scientific, ND-1000).

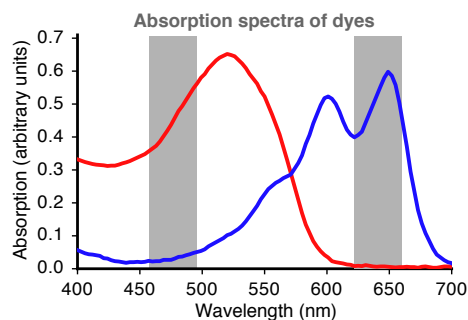


Figure S2: Plot of the absorption spectra of Oil Red O and Oil Blue N dyes in toluene. The regions of illumination for red and green light are shown shaded in grey.

To attach the ssDNA to the PS-PS-*b*-PEO- $\text{N}_3$  we mix 10  $\mu\text{L}$  of 70  $\mu\text{M}$  DBCO-modified ssDNA (IDT), 40  $\mu\text{L}$  of PS-PS-*b*-PEO- $\text{N}_3$  (1% v/v), and 150  $\mu\text{L}$  aqueous buffer containing

10 mM Tris and 1 mM EDTA (diluted to 1x TE from Serva TE Buffer (100x), pH 8) as well as 0.05% Pluronic F 127 (BASF) and 1 M NaCl. The solution is shaken for 24 h after which the mixture is washed with 1x TE several times.

### S3 Sample Preparation

To prevent oxidative damage to the DNA on the particles during illumination, we add a Glucose Oxidase/Catalase enzyme system that scavenges oxygen from the solution following the procedure in Ref. S3 (Section 3.2.3, pg 17). We mix 8  $\mu\text{L}$  1x TE with 625 mM NaCl, 1  $\mu\text{L}$  Glucose Oxidase/Catalase Stock (125 mM NaCl, 20 mg/mL Glucose Oxidase (from *Aspergillus niger*, Type VII, lyophilized powder, Sigma) and 3.5 mg/mL Catalase (Lyophilized, Spectrum) in 1x TE), and 0.1  $\mu\text{L}$  340 nm carboxylate-modified latex particles (Opti-Link, Thermo) and leave to react for 15 min. We separately prepare a 30  $\mu\text{L}$  suspension of 0.1% v/v PS-PS-*b*-PEO-DNA particles at 500 mM NaCl in 1x TE. We then add 1  $\mu\text{L}$  450 mg/mL D(+) Glucose (99.5%, Sigma) in DI water to our solution containing Glucose Oxidase/Catalase. We add 0.6  $\mu\text{L}$  of the resulting solution to the particle suspension.

We sprinkle 10–30  $\mu\text{m}$  glass spacer beads (Polysciences) onto a 24  $\times$  60 mm No. 1 coverslip and then plasma clean that and a 22  $\times$  22 mm No. 1 coverslip for 45 s. We place 20  $\mu\text{L}$  of the final solution onto the 24  $\times$  60 No. 1 coverslip and gently cover with the 22  $\times$  22 No. 1 coverslip, taking care to avoid trapping bubbles. We wick away the excess solution with a Kimwipe and seal the edges with UV-curable optical adhesive (Norland 63). Finally we cure the sample under UV for 5 min, keeping the center of the sample covered with aluminum foil.

### S4 Imaging

The methods used to heat and image are described in Refs. S4 and S1. Wide-field, wavelength-dependent illumination is provided by a Lumencor Spectra-X light engine. The illumination

power at the sample, as measured with a power meter at the back aperture of the objective, is 95 mW for green light (560/32 nm), 21.7 mW for red light (648 nm), and 32 mW for blue light (485/25 nm). The light is incident on an area of approximately  $(100 \mu\text{m})^2$  at the sample. For experiments comparing the response of samples illuminated with both red and blue light (see Figure 5), we make the illumination intensities the same by decreasing the power of the blue light to match that of the red light source.

## S5 Calculating heat profiles

Temperature profiles for a heated polystyrene bead are calculated following the method in Ref. S5. We assume a single bead in an infinite medium of water that perfectly absorbs  $3 \text{ MW/m}^2$  (which corresponds to the approximate true illumination intensity) of light, which it then perfectly radiates as heat.

The time-dependent results for the change in temperature  $T$  above the background are

$$T = \frac{a^2 A}{K_s} \left[ \frac{1}{3} \frac{K_s}{K_w} + \frac{1}{6} \left( 1 - \frac{r^2}{a^2} \right) - \frac{2ab}{r\pi} \int_0^\infty \frac{e^{-y^2 t / \gamma_s}}{y^2} \frac{(\sin y - y \cos y) \sin(ry/a)}{[(c \sin y - y \cos y)^2 + b^2 y^2 \sin^2 y]} dy \right], \quad (1)$$

if  $r \leq a$ , and

$$T = \frac{a^3 A}{r K_s} \left[ \frac{1}{3} \frac{K_s}{K_w} - \frac{2}{\pi} \int_0^\infty \frac{e^{-y^2 t / \gamma_s}}{y^3} \frac{(\sin y - y \cos y) [by \sin y - y \cos \sigma y - (c \sin y - y \cos y) \sin \sigma y]}{[(c \sin y - y \cos y)^2 + b^2 y^2 \sin^2 y]} dy \right] \quad (2)$$

if  $r \geq a$ . Here  $a$  is the particle radius ( $0.5 \mu\text{m}$ ),  $K_s$  is the thermal conductivity of polystyrene ( $0.4 \text{ W/m/K}$ ),  $K_w$  is the thermal conductivity of water ( $0.6 \text{ W/m/K}$ ),  $\rho_s$  is the density of polystyrene ( $1055 \text{ kg/m}^3$ ),  $\rho_w$  is the density of water ( $1000 \text{ kg/m}^3$ ),  $c_s^v$  is the heat capacity

of polystyrene (1300 J/kg/K),<sup>S6</sup>  $c_w^v$  is the heat capacity of water (4185.5 J/kg/K),  $k_s$  is the thermal diffusivity of polystyrene ( $k_s = K_s/(\rho_s c_s^v)$ ),  $k_w$  is the thermal diffusivity of water ( $k_w = K_w/(\rho_w c_w^v)$ ),  $A$  is the heat generated in the particle per unit volume per unit time (4.5 TW/m<sup>3</sup> assuming 10% of light incident on the 1  $\mu\text{m}$  particle is absorbed and perfectly re-radiated as heat) and

$$\begin{aligned}
 b &= \frac{K_w}{K_s} \sqrt{\left(\frac{k_s}{k_w}\right)} \\
 c &= 1 - \frac{K_w}{K_s} \\
 \gamma_s &= \frac{a^2}{k_s} \\
 \sigma &= \left(\frac{r}{a} - 1\right) \sqrt{\frac{k_s}{k_w}}.
 \end{aligned} \tag{3}$$

The steady-state results are

$$T = \frac{a}{6K_s} \left( a^2 - r^2 + 2a^2 \frac{K_s}{K_w} \right) \tag{4}$$

if  $r \leq a$ , and

$$T = \frac{Aa^3}{3K_w r} \tag{5}$$

if  $r \geq a$ . A plot of the steady-state result is shown in Figure S3. The time-dependent equations predict that for the conditions given above, the temperature should reach 99% of the steady-state value within 5 ms. The same equations predict that a 10  $\mu\text{m}$  particle should take 1 s to reach steady state, but only 1  $\mu\text{s}$  to heat by 1  $^\circ\text{C}$ .

## S6 Aggregation and diffusion time

In Figure 2 of the main text, we show the expansion of a cluster of particles exposed to light for 5 s. We then compare the observed expansion with the estimated expansion from a

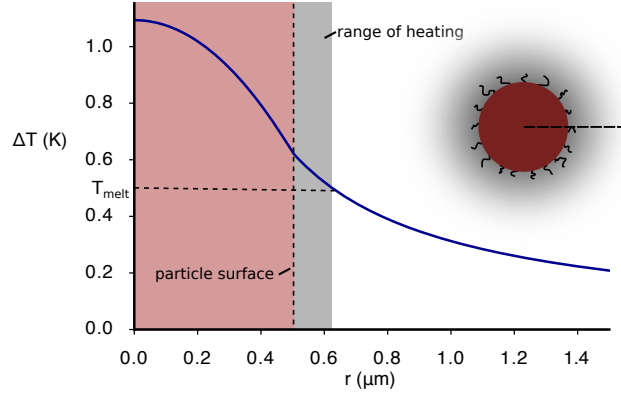


Figure S3: Theoretical calculation of the steady-state temperature profile of a dyed 1  $\mu\text{m}$  polystyrene particle in an infinite medium of water under exposure to light that the dye absorbs. The amount of heating depends on the power of illumination and the absorptivity of the dye in the wavelength used.

diffusion model:<sup>S7,S8</sup>

$$\begin{aligned} \langle x^2 \rangle &= 6Dt \\ D(T) &= \frac{k_B T}{6\pi\eta a} \\ \eta(T) &= 2.414 \times 10^{-5} \text{ Pa} \cdot \text{s} 10^{247.8 \text{ K}/(T-140 \text{ K})} , \end{aligned} \quad (6)$$

where  $\eta$  is the viscosity of water,  $D$  is the diffusion coefficient,  $a$  is the particle radius (0.5  $\mu\text{m}$ ),  $k$  is the Boltzmann constant ( $1.38 \times 10^{-23} \text{ m}^2 \text{ kg}/(\text{s}^2 \text{ K})$ ), and  $T$  is the temperature (318 K).

To calculate the expected time for a cluster of particles to aggregate, as shown in Figure 2a (last three panels), we assume that the limiting timescale is that for the particles on the outer edge of the cluster to diffuse inward and bind to those in the center. We estimate this distance to be 10  $\mu\text{m}$  by examining the third and last frames of Figure 2a. We then use Equations 6 to calculate the average time required to diffuse this distance.

## S7 Dimer melting experiments and analysis

For the dimer melting experiments, we make a sample as described in Section S3, except that we use 2  $\mu\text{m}$  particles to increase the amount of heating per particle, we work at lower volume fraction, and we make the sample quasi-two-dimensional. To do this, we forgo the use of spacer beads, place only 10  $\mu\text{L}$  of sample on the slide, and squeeze the two slides together using binder clips while curing the epoxy.

To make the sample, we mix 38  $\mu\text{L}$  1x TE with 263 mM NaCl and 0.1% F127, 1  $\mu\text{L}$  Glucose Oxidase/Catalase stock, and 0.1  $\mu\text{L}$  340 nm carboxyl-modified latex particles and wait 15 min. We separately prepare an 18  $\mu\text{L}$  suspension of 0.05% v/v PS-PS-*b*-PEO-DNA particles at 250 mM NaCl in 1x TE and place the suspension in a 55  $^{\circ}\text{C}$  water bath to keep the particles from aggregating. We then add 1  $\mu\text{L}$  glucose stock to the Glucose Oxidase/Catalase solution and 2  $\mu\text{L}$  of the resulting mixture to the particle suspension.

We place this sample on the heating stage and image it as described above. We bring the sample to just above the melting temperature and then use optical tweezers (785 nm) to drag approximately 20 single particles to an empty space in the sample. We then lower the temperature to approximately 10  $^{\circ}\text{C}$  below the melting temperature and assemble the single particles into dimers in a 3 by 3 grid with as much space between the dimers as possible within the field of view (see Figure S4). We then raise the temperature to 3  $^{\circ}\text{C}$  below the temperature at which most dimers break apart within a few seconds, even in the absence of illumination.

We use a CMOS Photon Focus camera with the frame rate set to 50 frame/s with an exposure time of 13.336 ms. We trigger the Lumencor light source with a square pulse of a given length (5 ms to 200 ms) with a period of 1 s. We record for 3000 frames (60 pulses). The light source and camera are not synchronized.

We repeat the experiment 9 times at each pulse length on the same set of 9 dimers. We rebuild the dimers using the optical tweezers between each experiment.

We post-process the micrographs to locate dimers and determine how many dimers break

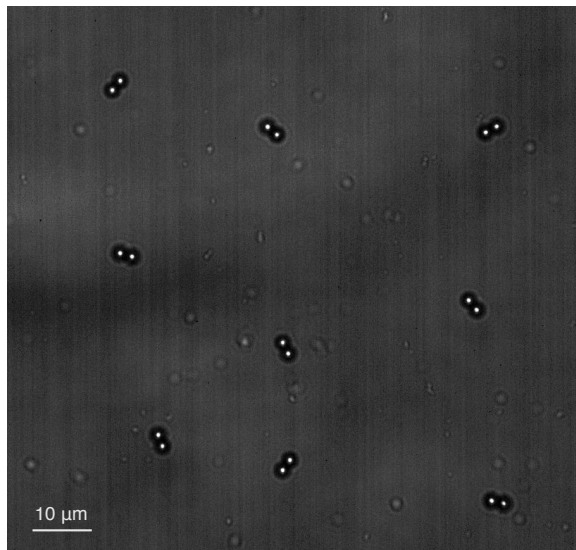


Figure S4: Three by three grid of dimers used to measure the response to different length pulses of light.

after a given light pulse using TrackPy,<sup>S9</sup> an open-source software package that is based on the Crocker-Grier centroiding algorithm.<sup>S10</sup> To set the TrackPy parameters, we identify particles in micrographs of dimers well below the melting temperature. We plot the particle positions from TrackPy on top of the micrographs and verify their locations by eye. By iterating over a range of TrackPy parameters, we optimize the particle positions while eliminating points that TrackPy falsely identifies as particles. We then use TrackPy to locate particles in space and time for the duration of the movie. TrackPy assigns each particle a unique identification number that allows us to associate particles between frames.

To identify which particles are bound together, we locate the particles and then classify particles as bound or unbound using a cutoff distance  $d_b$ . Particles that are less than  $d_b$  apart are said to be bound. We run the analysis for several different cutoff distances (see Figure S5).

We use a cutoff distance of  $d_b = 20.75$  pixels ( $2.21 \mu\text{m}$ ) for the analysis presented in the main text. This value is chosen by tracking dimers that are well below their melting temperature and measuring the distribution of interparticle separations at each of the over 3000 frames (see Figure S6). The  $3\sigma$  value is 20.75 pixels or, equivalently,  $2.21 \mu\text{m}$ .

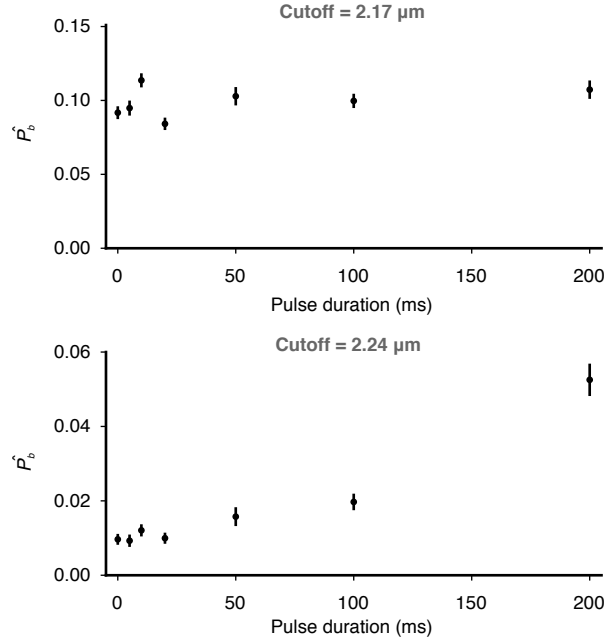


Figure S5: Analysis of dimer breaking probabilities at different particle separation cutoffs. Error bars correspond to a 1- $\sigma$  credible interval. See also Figure 4 of the main text.

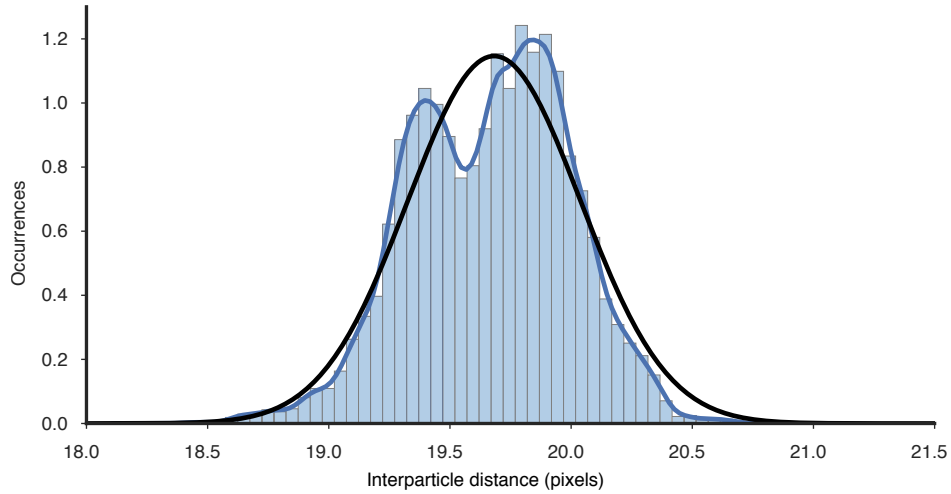


Figure S6: Distance between particles that are bound in dimers. Occurrences are counted over 3000 frames. The histogram is overlaid with a kernel density estimation (blue line), and fit to a Gaussian with the form  $a \exp(x - x_o)^2 / (2w)^2$  (black line). The fit values are  $a = 1.1466$ ,  $x_o = 19.6825$ ,  $w = 0.3560$ .

For each movie, we identify the frame before the  $i$ th light pulse ( $f_{\text{init},i}$ ) by eye. We calculate the separation between all pairs of particles in this frame and identify which particles are bound to only one other particle. This pair of particles is classified as a dimer; it is uniquely identified by the constituent particles' identification numbers.

To determine whether these dimers break, we calculate their interparticle distances for all frames in the movie after the  $i$ th pulse and before the  $(i + 1)$ th pulse. If the particle separation ever exceeds the cutoff distance  $d_b$ , we count the dimer as unbound. We repeat this procedure for every light pulse  $i$  in the movie.

We discard the frames when the light pulse is visible by eye because the images become saturated and the particle center tracking is unreliable. Thus, the total time we watch the dimers varies with the pulse length, with longer pulse lengths being analyzed for fewer frames. As a result, we may underestimate the number of breaking events at longer pulse lengths.

To show that the system is not heating over the course of each experiment, we plot the number of dimers present in the system before each light pulse for a movie containing 60 light pulses (see Figure S7). We see dimers re-forming after some of the pulses, and there is little evidence for long-term drift.

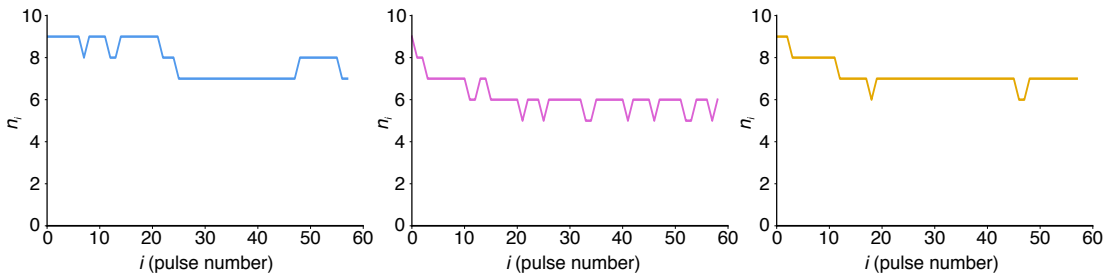


Figure S7: Number of dimers  $n_i$  present immediately preceding each pulse  $i$ , plotted for 3 different movies, recorded for 100 ms pulses with a cutoff distance of  $2.21 \mu\text{m}$ .

To extract a timescale for how quickly the light modulates the interactions, we infer the probability  $P_b$  (plus uncertainty) of a dimer breaking anytime after the pulse and before the next. Then, by plotting  $P_b$  as a function of pulse width, we can determine what pulse widths

have an effect on the melting of the dimers. We calculate the uncertainty on  $P_b$  to determine at what pulse width the effect becomes statistically significant.

We therefore determine the posterior probability distribution

$$p(P_b | \mathbf{D}, d_b) , \tag{7}$$

where  $\mathbf{D} = \{(b_1, n_1), (b_2, n_2), \dots, (b_l, n_l)\}$ ,  $n_i$  is the number of dimers present immediately before light pulse  $i$ ,  $b_i$  is the number of dimers that break between pulse  $i$  and  $i + 1$ , and  $l$  is the total number of pulses in all the movies for a particular pulse width. The posterior probability distribution gives us all of the information that the data contain about  $P_b$ , given our assumptions.

From Bayes's rule, the posterior probability is related to the product of the prior probability  $p(P_b)$  and the likelihood function  $p(\mathbf{D} | P_b, d_b)$ :

$$p(P_b | \mathbf{D}, d_b) = \frac{p(P_b) p(\mathbf{D} | P_b, d_b)}{p(\mathbf{D} | d_b)} , \tag{8}$$

where the denominator is a normalization factor. We retain the  $d_b$  on the right side of the “given” symbol ( $|$ ) because our calculations are conditioned on the threshold we choose.

We use a uniform prior for  $P_b$ ; that is,

$$p(P_b) = \begin{cases} 1 & 0 < P_b < 1 \\ 0 & \text{otherwise} . \end{cases}$$

This prior represents complete ignorance of  $P_b$ . We choose this prior because we don't have a good estimate of  $P_b$  before doing the experiment: even with no light pulses,  $P_b$  depends on many variables that are not precisely measured, such as the volume fraction of dimers in the system and the interaction between the particles at the temperature of the experiment.

We assume that all the measurements are independent. That is, each dimer breaks

(or does not break) independently of the others in a given pulse. Also, we assume no correlation between the measured fraction of broken dimers at pulse  $i$  and that at pulse  $j$ . We also assume that each pair of particles has the same interaction potential. In the actual experiment, there may be some heterogeneity in the interaction potential, such that the dimers that don't melt on a given pulse are those with a stronger interaction. We do not account for such heterogeneity in this simple estimation procedure.

With these assumptions, we can write down a likelihood function for the number of broken dimers after one pulse. The likelihood is a binomial distribution, since there are two possible outcomes for each dimer (broken or not broken), and each dimer is independent:

$$p(b_i, n_i | P_b, d_b) = \frac{n_i!}{b_i! (n_i - b_i)!} P_b^{b_i} (1 - P_b)^{n_i - b_i}. \quad (9)$$

Since each measurement at each pulse is independent, the likelihood of the entire data set (all the pulses in all the movies at a given pulse width) is the product of likelihood functions for a single pulse:

$$p(\mathbf{D} | P_b, d_b) = \prod_{i=1}^l p(b_i, n_i | P_b, d_b). \quad (10)$$

Because we have a uniform prior, the posterior probability distribution is proportional to the likelihood function:

$$p(P_b | \mathbf{D}, d_b) \propto p(\mathbf{D} | P_b, d_b). \quad (11)$$

Substituting our expression for the likelihood function into the above equation, we obtain

$$p(P_b | \mathbf{D}, d_b) \propto \prod_{i=1}^l \frac{n_i!}{b_i! (n_i - b_i)!} P_b^{b_i} (1 - P_b)^{n_i - b_i}. \quad (12)$$

We can then group terms in the product:

$$p(P_b | \mathbf{D}, d_b) \propto \left[ \prod_{i=1}^l \frac{n_i!}{b_i! (n_i - b_i)!} \right] P_b^{\sum_i b_i} (1 - P_b)^{\sum_i n_i - b_i}. \quad (13)$$

The term in brackets is a constant that depends only on the data. We ignore it because it becomes part of the normalization factor. If we then define

$$S_b = \sum_{i=1}^l b_i \quad (14)$$

and

$$S_{nb} = \sum_{i=1}^l (n_i - b_i), \quad (15)$$

the posterior probability becomes

$$p(P_b | \mathbf{D}, d_b) \propto P_b^{S_b} (1 - P_b)^{S_{nb}}. \quad (16)$$

This posterior probability distribution is a beta distribution. The beta distribution of  $x$ ,  $0 < x < 1$ , has two parameters,  $\alpha$  and  $\beta$ , where  $\alpha, \beta > 0$ :

$$p(x | \alpha, \beta) = \frac{\Gamma(\alpha + \beta)}{\Gamma(\alpha)\Gamma(\beta)} x^{\alpha-1} (1 - x)^{\beta-1}. \quad (17)$$

Here  $\Gamma$  is the gamma function,  $x = P_b$ ,  $\alpha = S_b + 1$ , and  $\beta = S_{nb} + 1$ .<sup>S11</sup>

We can analytically calculate the best estimate for  $P_b$ ,  $\hat{P}_b$ , and the uncertainty on that estimate from the known properties of the beta distribution. There are several possible choices for our estimator: we might use the mean of the distribution, its maximum (or mode), or its median. We choose the mean for our estimate and the standard deviation to characterize the uncertainty because there are analytical formulas for both. First, though, we note that the mean can be different from the maximum value of the distribution (the maximum *a posteriori* value or MAP, or mode) which is:<sup>S12</sup>

$$\text{MAP} = \frac{\alpha - 1}{\alpha + \beta - 2} = \frac{\sum_{i=1}^l b_i}{\sum_{i=1}^l n_i} = \frac{S_b}{S_n}, \quad (18)$$

where

$$S_n = \sum_{i=1}^l n_i. \quad (19)$$

The MAP value makes sense as an estimate of  $P_b$ : it is the total number of dimers that break divided by the total number of dimers. But because the beta distribution can be skewed, the mean value need not correspond to the MAP. The mean value, which we will use as our estimate  $\hat{P}_b$ , has the form<sup>S11</sup>

$$\hat{P}_b = \frac{\alpha}{\alpha + \beta} = \frac{1 + \sum_{i=1}^l b_i}{2 + \sum_{i=1}^l n_i} = \frac{1 + S_b}{2 + S_n}. \quad (20)$$

If the sums are large, there is little difference between the MAP and the mean. The advantage of using the mean is that we can use an analytical formula for the variance to estimate the uncertainty about the mean. The variance is:<sup>S12</sup>

$$\sigma_{P_b}^2 = \frac{\alpha\beta}{(\alpha + \beta)^2(\alpha + \beta + 1)} = \frac{(1 + S_b)(1 + S_{nb})}{(2 + S_n)^2(3 + S_n)}. \quad (21)$$

Thus, we estimate the uncertainty from the limits of a 1- $\sigma$  credible interval. The interval is

$$(\hat{P}_b - \sigma_{P_b}) < \hat{P}_b < (\hat{P}_b + \sigma_{P_b}). \quad (22)$$

## S8 Movies

Movie S1: Optical video of an aggregate of 1  $\mu\text{m}$  particles infiltrated with Oil Red O dye. The aggregate is held at a background temperature of 45 °C (3 °C below its melting temperature) and is exposed intermittently to 560 nm light (depicted by green border). The scale bar is 10  $\mu\text{m}$ . This movie corresponds to the still frames from Figure 2 in the main text.

## References

- (S1) Gehrels, E. W.; Rogers, W. B.; Manoharan, V. N. Using DNA strand displacement to control interactions in DNA-grafted colloids. *Soft Matter* **2018**, *14*, 969–984.
- (S2) Oh, J. S.; Wang, Y.; Pine, D. J.; Yi, G.-R. High-Density PEO-b-DNA Brushes on Polymer Particles for Colloidal Superstructures. *Chemistry of Materials* **2015**, *27*, 8337–8344.
- (S3) Collins, J. W. Self-Assembly of Colloidal Spheres with Specific Interactions. Ph.D. thesis, Harvard University, 2014.
- (S4) Rogers, W. B.; Manoharan, V. N. Programming colloidal phase transitions with DNA strand displacement. *Science* **2015**, *347*, 639–642.
- (S5) Goldenberg, H.; Tranter, C. J. Heat flow in an infinite medium heated by a sphere. *British Journal of Applied Physics* **1952**, *3*, 296.
- (S6) Gaur, U.; Wunderlich, B. Heat Capacity and Other Thermodynamic Properties of Linear Macromolecules. V. Polystyrene. *Journal of Physical and Chemical Reference Data* **1982**, *11*, 313–325.
- (S7) Einstein, A. On the movement of small particles suspended in stationary liquids required by the molecular-kinetic theory of heat. *Annalen der Physik* **1905**, *17*, 549–560.
- (S8) Kestin, J.; Sokolov, M.; Wakeham, W. A. Viscosity of liquid water in the range -8 °C to 150 °C. *Journal of Physical and Chemical Reference Data* **1978**, *7*, 941–948.
- (S9) Allan, D.; Caswell, T. A.; Keim, N.; Boulogne, F.; Perry, R. W.; Uieda, L. trackpy: Trackpy v0.2.4. 2014; doi: 10.5281/zenodo.12255.
- (S10) Crocker, J. C.; Grier, D. G. Methods of Digital Video Microscopy for Colloidal Studies. *Journal of Colloid and Interface Science* **1996**, *179*, 298–310.

- (S11) Gregory, P. *Bayesian Logical Data Analysis for the Physical Sciences*; Cambridge University Press, 2005.
- (S12) D'Agostini, G. *Bayesian Reasoning in Data Analysis: A Critical Introduction*; World Scientific, 2003.